Bistable polymer-stabilized cholesteric-liquid-crystal window based on flexoelectric and dielectric effects

Ziyuan Zhou,[1] Xinfang Zhang,[1] Suman Halder,[2] Lang Hu,[1] and Deng-Ke Yang[1,2,*]

[1] *Materials Science Graduate Program, Advanced Materials and Liquid Crystal Institute, Kent State University, Kent, Ohio 44242, USA*

[2] *Department of Physics, Kent State University, Kent, Ohio 44242, USA*

(Received 9 November 2023; revised 3 January 2024; accepted 5 February 2024; published 23 February 2024)

Smart switchable windows for buildings and vehicles become more and more important because they can reduce energy consumption. They exhibit two optically contrasting states: a transparent state and an optically scattering (or light-absorbing) state. Most of them are, however, monostable, namely, only one of the optical states is stable in the absence of applied voltage, and the other state must be sustained under continuously applied voltage, which would consume energy. Here, we report a bistable smart window based on polymer-stabilized cholesteric liquid crystals. The window exhibits two stable states at 0 V: one of them is the transparent homeotropic state with a high transmittance and the other state is the scattering focal conic state with a low transmittance. The bistable states are achieved by using an anisotropic polymer network, known as polymer stabilization. The window is switched from the transparent state to the scattering state by a low-frequency ac voltage pulse under the flexoelectric effect and is switched from the scattering state back to the transparent state by a high-frequency ac voltage pulse under the dielectric interaction. No voltage is needed to sustain the two states of the window. Therefore, the window almost does not consume energy. The optical contrast between the two states is high, and the window is very efficient at privacy control. Due to its superior performance and very low energy consumption, this technology is expected to have a significant impact on switchable architectural and automobile windows.

DOI: 10.1103/PhysRevApplied.21.024045

I. INTRODUCTION

There has been intensive research on smart switchable windows in the last couple of decades. They are used to control privacy and (or) solar-energy flow and are widely used in architectural buildings, automobiles, and airplanes. They can provide a comfortable environment and reduce energy consumption by minimizing the need for excessive air conditioning [1–7]. Current technologies used for smart windows are a suspended particle device [8,9], liquid crystals (LCs) [10–13], and electrochromics [14–16]. Among these technologies, LC smart windows have received significant attention due to their distinctive optical properties, low manufacturing cost, and fast switching time. There are several types of smart windows based on liquid crystals, such as polymer-dispersed liquid crystals (PDLCs) [17–23], polymer-stabilized liquid crystals [24–28], and polymer-stabilized cholesteric texture (PSCT) [29–35]. A PDLC consists of approximately equal amounts of nematic liquid crystal and polymer [36,37]. The liquid crystal is optically anisotropic and exhibits an ordinary refractive index, n_o, for light polarized perpendicular to the average direction of the long axis of the elongated liquid-crystal molecule and an extraordinary refractive index, n_e, for light polarized parallel to the average direction. The polymer is optically isotropic and exhibits a refractive index, n_p, that is matched to n_o. The liquid crystal forms micron-sized droplets, which are dispersed in the polymer. In the absence of an applied voltage, the orientation of the liquid-crystal droplets is random. When light propagates through the PDLC film, it encounters the refractive index, n_p, in the polymer, but a different refractive index, which is between n_o and n_e, in the liquid-crystal droplets. Thus, the light is scattered and the PDLC film appears opaque. When a voltage is applied across the film, the liquid-crystal droplets are aligned along the film's normal direction. A normal incident light encounters the same refractive index in the polymer and liquid-crystal droplets. Thus, the light is not scattered and the film becomes transparent. A PSCT is made from a composite consisting of a cholesteric liquid crystal (CLC) of high concentration (∼90%) and a polymer network of low concentration (∼10%). Both the liquid crystal and polymer network are optically anisotropic. In a normal-mode PSCT, the polymer network is perpendicular to the PSCT film and is dispersed in the liquid crystal and has an aligning effect on the liquid crystal. The

*dyang@kent.edu

cholesteric liquid crystal has a helical structure, where the liquid-crystal molecules twist around a helical axis. In the absence of an applied voltage, the liquid crystal is in a random polydomain state, known as a focal conic texture, where the directions of the helical axes of the domains are random, due to the dispersed polymer network. When light propagates through the PSCT film, it encounters different refractive indices in different domains. Therefore, light is scattered and the film appears opaque. When a voltage is applied across the film, the helical structure is unwound and the liquid crystal is aligned along the film's normal direction, parallel to the polymer network. Therefore, light is not scattered and the film becomes transparent.

As aforementioned, for most of the smart windows, voltages must be applied to sustain their optical state, which consumes energy. To save energy, it is highly desirable that a smart window should have two optically contrasting states at 0 V and can be switched between the two states by voltage pulses. Several technologies have been developed to fulfill the goal. Moheghi *et al*. [38] developed bistable CLC windows in which the two stable states were the transparent planar texture (state), where the helical axis was uniformly aligned perpendicular to the window film, and the scattering focal conic texture (state). The CLCs used have negative dielectric anisotropies and are doped with ions. When a relatively high-frequency ($\sim$1 kHz) voltage pulse is applied, the materials are switched from the focal conic texture to the planar texture under a dielectric interaction, while, when a low-frequency ($\sim$10 Hz) voltage pulse is applied, the materials are switched from the planar texture to the focal conic texture due to the turbulent motion of the ions. The technology has, however, a problem because the doped ions cause degradation of the liquid crystal. Lin's group developed a CLC window where two of the tristable states were the transparent planar texture and scattering focal conic texture [39]. The window also has an undesirable feature because a complicated electrode structure has to be used. Ma *et al*. [40] developed a bistable polymer-stabilized CLC window operated between the transparent homeotropic texture and scattering focal conic texture. A polymer network with a strong aligning effect is used to stabilize the homeotropic texture at 0 V. The CLC used is a dual-frequency LC. When a low-frequency (lower than 10^2 Hz) voltage is applied, the LC exhibits a positive dielectric anisotropy and tends to align parallel to the applied electric field, while, when a high-frequency (higher than 10^4 Hz) voltage is applied, the LC exhibits a negative dielectric anisotropy and tends to align perpendicular to the applied electric field. When a low-frequency voltage pulse is applied, the CLC is switched from the focal conic texture to the homeotropic texture. When a high-frequency voltage pulse is applied, the CLC is switched from the homeotropic texture to the focal conic texture. There are, however, a few issues with the dual-frequency liquid crystal. First of all, the frequency of the high-frequency voltage pulse is very high ($\sim$10 kHz). The window is essentially a capacitor, and the power needed to switch the window is high due to the high frequency of the voltage. Second, the required high frequency changes dramatically with temperature [41,42]. Third, the magnitude of the negative dielectric anisotropy under the high-frequency voltage is small, and thus, the driving voltage is high. Furthermore, there are only a very few commercially available dual-frequency liquid crystals.

Here, we report a bistable smart window based on a polymer-stabilized cholesteric texture. It has two stable states at 0 V: the transparent homeotropic state and the scattering focal conic state. It is switched from the focal conic state to the homeotropic state by a high-frequency (1 kHz) voltage pulse under the dielectric interaction, and it is switched from the homeotropic state to the focal conic state by a low-frequency (10 Hz) voltage pulse under the flexoelectric interaction. The required frequencies do not change with temperature. Furthermore, high transmittance of the transparent state and low transmittance of the scattering state are achieved.

II. OPERATION PRINCIPLE

The bistable PSCT window is made from liquid crystal and polymer network composite. The liquid crystal is a CLC, which possesses an intrinsic helical structure where the LC twists periodically around a helical axis. The distance along the helical axis for the LC to rotate 360° is the pitch, denoted by P. The CLC has a positive dielectric anisotropy and interacts with an externally applied electric field, $\vec{E}$, under the dielectric interaction, the energy density of which is given by

$$f_{\text{dielectric}} = -\frac{1}{2}\varepsilon_o \Delta\varepsilon (\vec{n}\cdot\vec{E})^2, \tag{1}$$

where ε_o is the permittivity of free space, $\Delta\varepsilon$ is the dielectric anisotropy of the LC, and $\vec{n}$ is the LC director (a unit vector along the averaged direction of the long molecular axis). The dielectric interaction is not sensitive to the polarity of the applied electric field, and the interaction energy is proportional to the square of the applied electric field. Because $\Delta\varepsilon > 0$, the interaction energy is minimized when the LC is parallel or antiparallel to the electric field. When an ac voltage is applied across the CLC, the aligning effect on the LC of the electric field under the dielectric interaction does not depend on the frequency of the applied voltage (typically up to 10 kHz, below which the dielectric anisotropy remains the same), because the dielectric interaction is not sensitive to the polarity of the applied voltage. When the applied electric field is higher than $E_c = (\pi^2/P)\sqrt{K_{22}/\varepsilon_o\Delta\varepsilon}$ [43], where K_{22} is the twist elastic constant of the CLC, the helical structure is unwound under the dielectric interaction. The CLC also contains a liquid-crystal component of bent molecular shape and

exhibits the flexoelectric effect. When the director $\vec{n}$ is uniform in space, the CLC does not exhibit a net spontaneous electric polarization. When the director $\vec{n}$ is not uniform in space, but in a splay or bent director deformation, the CLC exhibits spontaneous polarization. Therefore, the CLC also interacts with the externally applied electric field through a flexoelectric interaction [44–48], the energy density of which is given by

$$f_{\text{flexoelectric}} = -\{e_s[\vec{n}(\nabla \cdot \vec{n})] + e_b[\vec{n} \times (\nabla \times \vec{n})]\} \cdot \vec{E}, \quad (2)$$

where e_s and e_b are the splay and bent flexoelectric coefficients, respectively. The energy of the flexoelectric interaction is linearly proportional to the applied electric field. The flexoelectric interaction energy is minimized when a spontaneous splay and bent deformation of the LC director is formed. Thus, the flexoelectric interaction tends to produce a nonuniform state of the LC. Note that the flexoelectric interaction is sensitive to the polarity of the applied voltage. When the polarity of the applied voltage is changed, the LC direction will be reversed. When an ac voltage is applied, the response of the LC under the flexoelectric interaction depends on the frequency of the applied voltage due to limited rotational mobility. When the frequency is low, typically less than 10^2 Hz, the LC is able to rotate sufficiently fast to follow the direction of the applied electric field. When the frequency is high, the LC is no longer able to rotate to follow the direction of the applied electric field, and thus, the flexoelectric interaction does not play a role in the determination of the LC state. Therefore, when an ac voltage of low frequency is applied, the state of the LC is determined by both the dielectric and flexoelectric interactions, while, when an ac voltage of high frequency is applied, the state of the LC is determined only by the dielectric interaction.

In the fabrication of the bistable window, initially, the CLC is mixed with a small amount of reactive monomers. The mixture is sandwiched between two parallel substrates with an indium tin oxide (ITO) transparent electrode. The material is irradiated by UV light to polymerize the monomers. During polymerization, a high-frequency voltage is applied between the top and bottom ITO electrodes. Through the dielectric interaction, the CLC is switched to the homeotropic state, where the helical structure is unwound and the LC molecules are aligned perpendicular to the substrates. Due to the aligning effect of the LC on the monomers, an anisotropic polymer network perpendicular to the substrates is formed, as shown in Fig. 1(a). The formed polymer network, in reverse, has an aligning effect on the LC [49,50], which tends to keep the CLC in the homeotropic state. The strength of the aligning effect depends on the chemical structure and concentration of the polymer network. If the aligning effect is sufficiently strong, the CLC will remain in the homeotropic state after the applied voltage is removed. When a low-frequency ac voltage is applied, the homeotropic state, where the LC orientation is uniform, becomes unstable due to the flexoelectric interaction, and the CLC is switched to the focal conic state, as shown in Fig. 1(b).

When the applied voltage is removed, although the polymer network has an aligning effect on the LC, it is not able to switch the CLC to the homeotropic state. Therefore, the CLC remains in the focal conic state. When the high-frequency ac voltage is applied again, the CLC is switched to the homeotropic state and remains in the homeotropic state after the removal of the applied voltage.

III. MATERIALS AND EXPERIMENT

In the construction of the CLC for the bistable PSCT window, the components were carefully chosen with

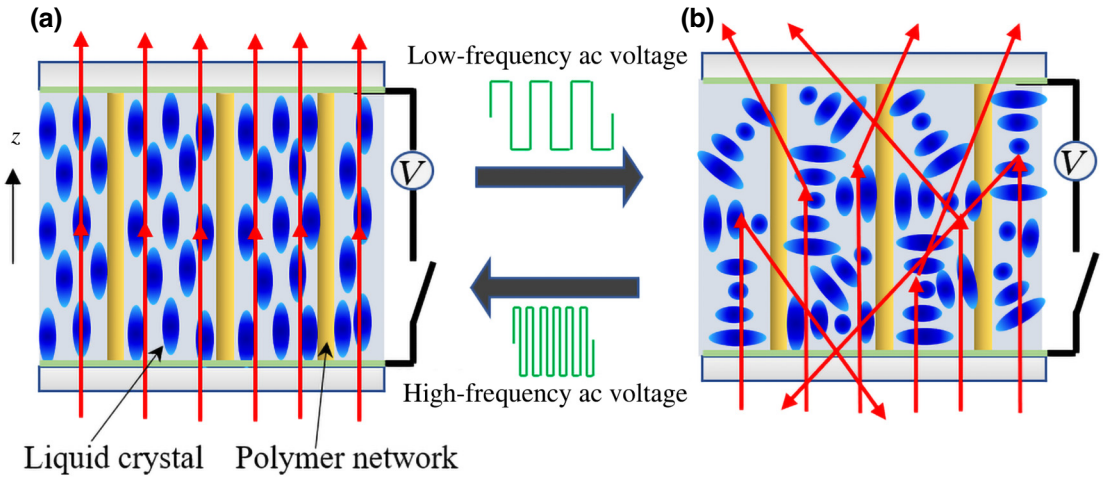

FIG. 1. Schematic diagram showing the operation of the bistable PSCT window. (a) Transparent homeotropic state, (b) scattering focal conic state.

the consideration of the following properties: flexoelectric coefficients, dielectric anisotropy, pitch length, and polymer-network concentration. The flexoelectric coefficients should be large, so that the required amplitude of the low-frequency voltage to switch the CLC to the focal conic state is low. The dielectric anisotropy must be positive, but not too large, so that the dielectric interaction is insignificant, and thus, the flexoelectric effect is dominant when the low-frequency voltage is applied, and not too small, so that the amplitude of the required high-frequency voltage to switch the CLC to the homeotropic state is not high. The pitch has profound effects on the stability of the homeotropic state and the scattering efficiency of the focal conic state. When the pitch is too short, the homeotropic state is unstable at 0 V. When the pitch is too long, the scattering of the focal conic state is weak. The polymer-network concentration also greatly affects the stability of the homeotropic state and the scattering efficiency of the focal conic state. When the polymer-network concentration is too low, the homeotropic state is unstable at 0 V. When the polymer-network concentration is too high, the scattering of the focal conic state is low. With the aforementioned considerations, the nematic host (NH) was made from 33.6 wt% HNG7058 (from HCCH), the dielectric anisotropy of which is −9; 13.5% E7 (from Merck), the dielectric anisotropy of which is +14; and 35.3% CB7CB and 17.6 wt% CB9CB (from HCCH), the dielectric anisotropies of which are about +2. HNG7058 and E7 are regular nematic liquid crystals and have a wide nematic phase temperature region. CB7CB and CB9CB were added to obtain a large flexoelectric coefficient. They are liquid-crystal dimers consisting of two mesogenic biphenyl groups at the two sides and a flexible hydrocarbon chain in the middle [51–54]. Because the number of carbon atoms in the hydrocarbon chain is odd, they have a bent shape. Furthermore, the mesogenic groups have a cyano group that has a permanent dipole. These dimers have large flexoelectric coefficients ($e_s + e_b$) of around −31 pC/m [55,56]. They are, however, not in the nematic phase at room temperature. They must be mixed with HNG7058 and E7 to obtain the nematic phase at room temperature. If only one of them is used, it cannot be doped enough to obtain a sufficiently large flexoelectric coefficient due to its limited solubility in HNG7058 and E7. The CLC was made from the NH and chiral dopant CB15. The helical twist power (HTP) of CB15 is about 8 μm^{-1}. The pitch of the CLC was adjusted by varying the chiral dopant concentration, x, according to $P = 1/(H \cdot x)$, where H is the helical twisting power (HTP) of the chiral dopant. CB15 also has a positive dielectric anisotropy. We made a mixture of 8 wt% CB15 and 92 wt% NH and measured the dielectric anisotropy (at 1 kHz) to obtain a value of +1.57. The CLC was then mixed with RM257 (from Merck), which is a mesogenic monomer. A small amount of the photoinitiator benzoin methyl ether (BME) was added. The concentration ratio between RM257 and BME was kept at around 4:1.

The cell used in our experiment was constructed from two parallel glass substrates with ITO coating (which serves as the transparent electrode). A homeotropic alignment layer of polyimide SE5661 (from Nissan Chemical) was spin coated on top of the ITO layer. Then the alignment layer was prebaked at 80 °C for 5 min and hard baked at 180 °C for 1 h. It was also mechanically rubbed with a cloth to generate a small pretilt angle. The alignment layer provides a homeotropic alignment of the LC on the surface. The cell thickness was controlled by 12-μm spacers. The mixture was transferred into the cell by capillary force at an elevated temperature. After cooling to room temperature, the cell was irradiated by UV light at an intensity of 10 mW/cm^2 for 1 h to polymerize the monomer. During polymerization, an ac voltage of 100 V and 1 kHz was applied, such that the helical structure of the CLC unwound and the LC molecules aligned perpendicular to the cell substrate.

The textures of the samples used in our experiments were studied under a polarizing optical microscope (Nikon, Optiphot2-POL) with crossed polarizers. A CCD camera (AmScope, MD900E) was mounted on the microscope to take microphotographs. The transmittance of the samples was measured with an unpolarized green He-Ne laser with a wavelength of 543 nm. The light was normally incident on the sample. The transmitted light was measured by a photodiode detector. The collection angle of the detector was 4°. The transmittance was obtained by normalizing the measured light intensity after the sample to the incident light intensity before the sample. When a low-frequency voltage was applied, the transmitted-light intensity oscillated with time due to the voltage-polarity sensitiveness of the flexoelectric interaction. The transmittance reported was the transmittance averaged over 1 s, unless otherwise specified.

IV. RESULTS

We first check whether the LC has a large flexoelectric coefficient and if its flexoelectric interaction with the electric field is strong. It is well known that a nematic LC with a large flexoelectric coefficient exhibits a periodic striped structure when a dc voltage is applied [57–60]. The LC used for our smart window is, however, a CLC and can exhibit a periodic striped structure due to its periodic helical structure, known as the fingerprint texture, in the presence of an externally applied electric field. It is difficult to determine whether the striped structure is caused by the flexoelectric effect or the periodic helical structure. To overcome the difficulty, we constructed a nematic LC from the CLC by adding another chiral dopant, S5011. The chiral dopant CB15 induces a right-handed helix and has a HTP of 8 μm^{-1}, while chiral dopant S5011 induces

a left-handed helix and has a HTP of $-130\ \mu m^{-1}$. When the concentration ratio between CB15 and S5011 is around 130:8, their helical twisting powers cancel each other out. We used this method to obtain a nematic LC, which consisted of 91.2% NH, 8.3% CB15, and 0.5% S5011. This nematic LC has the following phase behavior: it transforms from the isotropic phase to the nematic phase at 66.6 °C, and from the nematic phase to the twist-bend nematic phase at 30.7 °C. The material filled a 5-μm-thick and 1-inch^2 area cell with a homogeneous alignment layer. We studied the response of the nematic LC to an applied electric field in the nematic phase at 32 °C under the polarizing optical microscope. The results are shown in Fig. 2. The frequency of the applied voltage is 0 Hz. When the applied voltage is zero, the nematic LC is homogeneously aligned along the rubbing direction. Because the rubbing direction is parallel to the polarizer at the entrance plane, the incident light is linearly polarized parallel to the LC direction, and its polarization does not change when propagating through the LC layer. Light is absorbed by the analyzer at the exiting plane, and thus, the sample appears dark, as shown in Fig. 2(a). When the applied voltage is increased to 20 V, the LC is switched to a nonuniform state with spontaneous splay and bent deformations, due to the flexoelectric interaction, and the sample exhibits a periodic striped structure, as shown in Fig. 2(b). The direction of the stripe is parallel to the alignment-layer rubbing direction. When the applied voltage is increased to 22 V, the stripes start to wiggle, as shown in Fig. 2(c), which is probably caused by the dielectric interaction. When the voltage is increased to 50 V, the sample exhibits an irregular multidomain mosaic pattern texture, as shown in Fig. 2(d). No

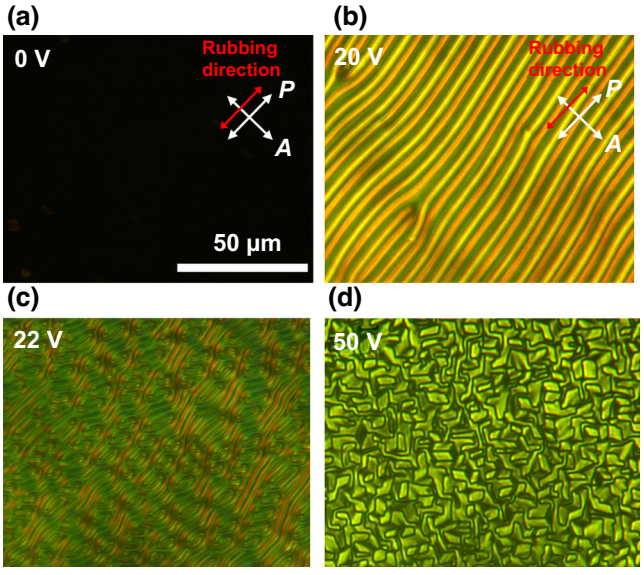

FIG. 2. Microphotographs of the nematic LC at 32 °C under various voltages. Rubbing direction is parallel to the polarizer of the microscope. Frequency of applied voltage is 0 Hz.

turbulence, a characteristic motion of ions, is observed. We also measured the resistance of the sample and found its resistance was 1.8 MΩ, i.e., very high. Therefore, it can be concluded that the periodic striped and irregular multidomain states are caused by the flexoelectric effect, but not by the electroconvective instability of nematic LCs with high ion concentrations.

A critical condition of the operation of the bistable window is that the polymer network has a sufficiently strong aligning effect on the CLC, so that the CLC is in the homeotropic texture after removal of the high-frequency voltage, but not too strong, so that the CLC is in the focal conic texture after the removal of the low-frequency voltage. The aligning effect of the polymer network is dependent on its concentration. The higher the concentration, the stronger the aligning effect becomes [50]. We made a few bistable samples, R1, R3, and R5, with a variety of polymer-network concentrations, as listed in Table I. The chiral dopant (CB15) concentration was fixed at 8%. The accuracy of the percentage of the components is 0.01%. We investigated the bistability of the samples under the polarizing optical microscope. The results for samples R1, R3, and R5 are shown in Fig. 3. For sample R1, the polymer-network concentration is 4.0%. When a voltage of 100 V (10 Hz) is applied, the CLC is in the focal conic state, the texture of which is shown in Fig. 3(a1). When the applied voltage is turned OFF, the CLC transforms into the homeotropic texture, the texture of which is shown in Fig. 3(a2). When the CLC is in the homeotropic texture, it does not change the polarization of the incident light, and thus, the texture is black. When the voltage of 100 V (1 kHz) is applied, the CLC is in the homeotropic state, the texture of which is shown in Fig. 3(a3). When the applied voltage is turned OFF, the CLC remains in the homeotropic texture, the texture of which is shown in Fig. 3(a4). Therefore, when the polymer-network concentration is 4%, the aligning effect is too strong. For sample R3, the polymer-network concentration is 3.6%. When the voltage of 100 V (10 Hz) is applied, the CLC is in the focal conic state, the texture of which is shown in Fig. 3(b1). When the applied voltage is turned OFF, the CLC remains in the focal conic texture, the texture of which is shown in Fig. 3(b2). When the voltage of 100 V (1 kHz) is applied, the CLC is in the homeotropic state, the texture of which is shown in Fig. 3(b3). When the applied voltage is turned OFF, the CLC remains in the homeotropic texture, the texture of which is shown in Fig. 3(b4). Therefore, when the polymer-network concentration is 3.6%, the aligning effect is properly strong. For sample R5, the polymer-network concentration is 3.0%. When the voltage of 100 V (10 Hz) is applied, the CLC is in the focal conic state, the texture of which is shown in Fig. 3(c1). When the applied voltage is turned OFF, the CLC remains in the focal conic texture, the texture of which is shown in Fig. 3(c2). When the voltage of 100 V (1 kHz) is applied, the CLC is in

TABLE I. Bistable samples with different concentrations of monomer RM257. FC, focal conic state; *H*, homeotropic state.

Sample No.	NH (wt %)	CB15 (wt %)	RM257 (wt %)	BME (wt %)	Transmittance of FC state at 0 V (%)	Transmittance of *H* state at 0 V (%)
R1	87.0	8.0	4.0	1.0	unstable	
R2	87.4	8.0	3.7	0.9	6.5	84.9
R3	87.5	8.0	3.6	0.9	2.0	84.4
R4	87.6	8.0	3.5	0.9	0.2	81.5
R5	88.2	8.0	3.0	0.8		unstable

the homeotropic state, the texture of which is shown in Fig. 3(c3). When the applied voltage is turned OFF, the CLC transforms into the focal conic texture, the texture of which is shown in Fig. 3(c4). Therefore, when the polymer-network concentration is 3%, the aligning effect is too weak.

We fine-tuned the polymer-network concentration to around 3.6%. We made two more bistable samples, R2 and R4, with concentrations close to 3.6, as listed in Table I. We measured the transmittance as a function of applied voltage of the bistable samples. When the CLC is initially in the homeotropic state and the frequency of applied voltage is 10 Hz, the results are shown in Fig. 4(a). For sample R2, the polymer-network concentration is 3.7%. Its transmittance is 84.9% at 0 V. Most of the light loss is caused by reflection from the interfaces of the cell. When the applied voltage is below a threshold voltage, $V_{H\to FC}$ (threshold voltage for the transition from the homeotropic state to the focal conic state), of 71 V, it remains in the homeotropic state with high transmittance. When the applied voltage is increased above the threshold, the CLC is gradually switched to the focal conic state and the transmittance starts to decrease. When the applied voltage is increased to 85 V, the minimum transmittance of 50% is obtained. When the applied voltage is increased further, the transmittance increases, probably because the dielectric interaction overtakes the flexoelectric interaction and suppresses the randomness of the focal conic state. When the applied voltage is decreased, the transmittance decreases, instead of increasing, indicating that the CLC remains in the focal conic state. When the voltage is decreased to 0, the CLC is still in the focal conic state with a transmittance of 6.5%. For sample R3, the polymer-network concentration is 3.6%. Its transmittance is 84.4% at 0 V. The threshold voltage to switch the CLC to the focal conic texture is 62 V, which is lower than that of sample R2. The lower

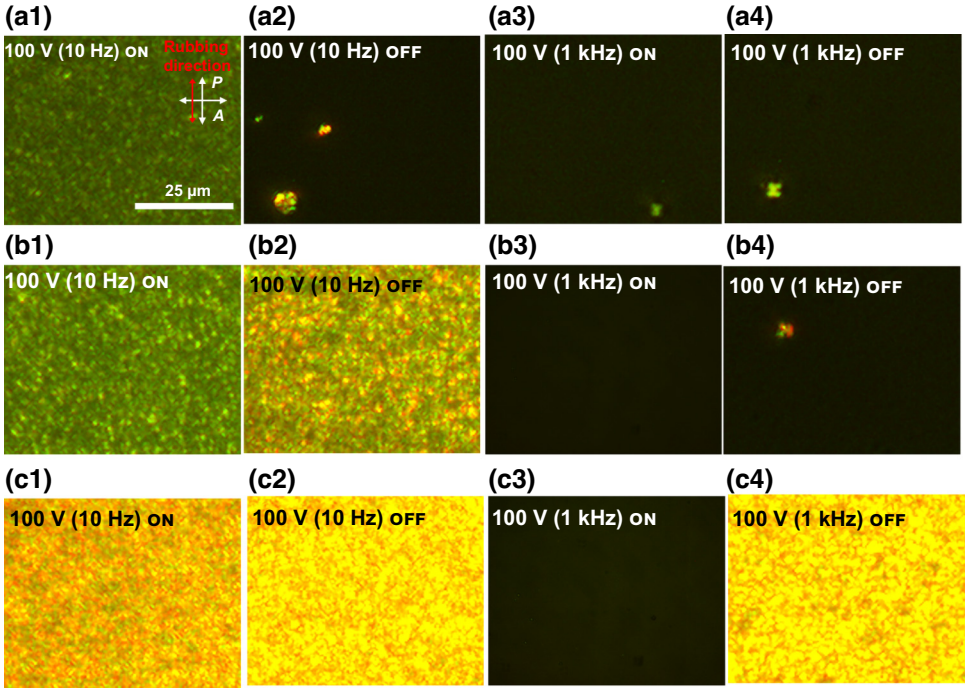

FIG. 3. Microphotographs of the bistable samples at 22 °C under voltages of different frequencies. Row 1, sample R1; row 2, sample R3; row 3, sample R5; column 1, 100 V (10 Hz) is turned ON; column 2, 100 V (10 Hz) is turned OFF; column 3, 100 V (1 kHz) is turned ON; column 4, 100 V (1 kHz) is turned OFF.

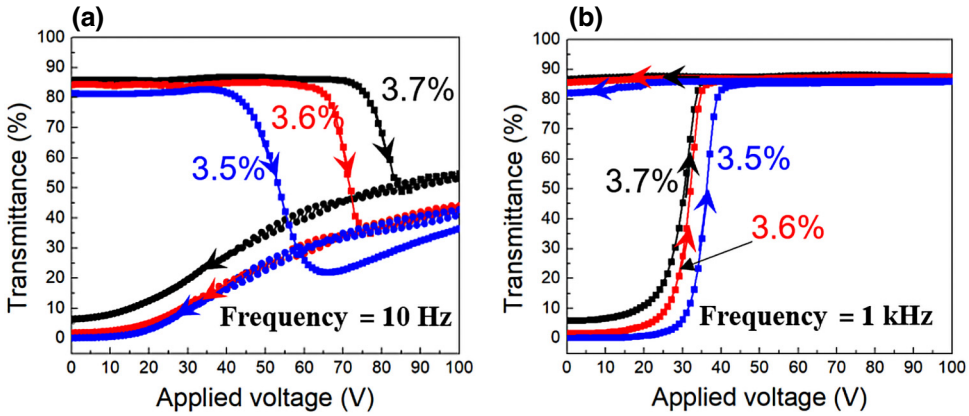

FIG. 4. Transmittance versus applied voltage curves of bistable samples with various polymer-network (RM257) concentrations. (a) Frequency of applied voltage is 10 Hz, (b) frequency of applied voltage is 1 kHz.

threshold voltage is because the aligning effect of the polymer network in sample R3 is lower than that of sample R2, and thus, a lower threshold voltage is needed to overcome the aligning effect of the polymer network. When the applied voltage is increased above 74 V and then removed, the CLC remains in the focal conic state. At 0 V, the transmittance is 2.0%, which is lower than sample R2, because of the weaker aligning effect of the polymer network. For sample R4, the polymer-network concentration is 3.5%. Its transmittance is 81.5% at 0 V, which is lower than those of samples R2 and R3. The decrease in transmittance is because the aligning effect of the polymer is weaker and it is not able to hold the CLC completely in the homeotropic state. The threshold voltage to switch the CLC to the focal conic texture is 42 V, which is lower than that of sample R3 because of the weaker aligning effect of the polymer. When the applied voltage is increased above 65 V and then removed, the CLC remains in the focal conic state. At 0 V, the transmittance is 0.2%, which is very low.

When the CLC is initially in the focal conic state and the frequency of the applied voltage is 1 kHz, the results are shown in Fig. 4(b). For sample R2, its transmittance is 6.5% at 0 V. When the applied voltage is below another threshold voltage, $V_{FC\rightarrow H}$ (threshold voltage for the transition from the focal conic state to the homeotropic state), of 10 V, it remains in the focal conic state with low transmittance. When the applied voltage is increased above the threshold, the size of the focal conic domain is gradually increased and the transmittance increases. When the applied voltage is increased above another threshold voltage of 35 V, the helical structure is unwound and the CLC is switched to the homeotropic texture with a maximum transmittance of 87%. When the applied voltage is increased further, the transmittance no longer changes. When the applied voltage is decreased, even if it is completely removed, the CLC remains in the homeotropic texture, due to the strong aligning effect of the polymer network, and the transmittance does not change. For sample R3, its transmittance is 2.0% at 0 V. The threshold voltage, at which the focal conic domain size begins to increase and simultaneously the transmittance starts to increase, is 15 V, which is higher than that of sample R2, because its polymer-network aligning effect is weaker than that of sample R2. The threshold voltage to switch the CLC to the homeotropic state is 36 V, which is slightly higher than that of sample R2. When the CLC is in the homeotropic state, the transmittance is 87%, which is the same as that of sample R2. When the applied voltage is decreased, even if it is completely removed, the transmittance does not change, because the aligning effect of the polymer is still strong enough to hold the CLC in the homeotropic state. For sample R4, its transmittance is 0.2% at 0 V. The threshold voltage, at which the focal conic domain size begins to increase and the transmittance starts to increase, is 20 V, which is higher than those of samples R2 and R3, because its polymer-network aligning effect is weaker than those of samples R2 and R3. The threshold voltage to switch the CLC to the homeotropic state is 40 V. When the CLC is in the homeotropic state, the transmittance is 86%, which is slightly lower than those of samples R2 and R3. When the applied voltage is decreased to 0, the transmittance decreases to 81.5%, because the aligning effect of the polymer network is not strong enough to hold the CLC completely in the homeotropic state and a small percentage of material transforms into the focal conic state.

The pitch of the CLC is another important factor controlling the electro-optical property of the bistable window. First, it affects the focal conic domain size, which, in turn, influences the scattering of the material. The shorter the pitch is, the stronger the scattering becomes. Second, the field (sum of the applied electric field and the aligning field of the polymer) needed to switch the CLC to the homeotropic texture is inversely proportional to the pitch. The pitch is determined by the concentration of chiral

TABLE II. Bistable samples with different concentrations of chiral dopant CB15.

Sample No.	NH (wt %)	CB15 (wt %)	RM257 (wt %)	BME (wt %)	Transmittance of FC state at 0 V (%)	Transmittance of *H* state at 0 V (%)
C1	90.3	6.0	3.0	0.7	5.4	81.4
C2 (R3)	87.5	8.0	3.6	0.9	2.0	84.4
C3	85.0	10.0	4.0	1.0	12.1	85.1

dopant CB15. We made three samples with different chiral dopant concentrations, as listed in Table II. To make the homeotropic texture stable at 0 V, the concentration of the polymer network was adjusted accordingly. When the CLC is initially in the homeotropic state and the frequency of the applied voltage is 10 Hz, the results are shown in Fig. 5(a). The low-frequency voltage is applied, so the CLC is switched from the homeotropic texture to the focal conic texture. When the voltage is turned OFF, the CLC remains in the focal conic texture. For sample C2, which is the same as sample R3, the chiral dopant concentration is 8%, and the corresponding pitch is $P = 1/[8\ \mu\text{m}^{-1} \times 0.08] = 1.6\ \mu\text{m}$. Its electro-optical property has already been discussed in the above paragraphs. For sample C1, the chiral dopant concentration is 6%, and the corresponding pitch is $P = 1/[8\ \mu\text{m}^{-1} \times 0.06] = 2.1\ \mu\text{m}$. Its transmittance is 81.4% at 0 V, probably because the polymer-network concentration is not high enough. The threshold voltage to switch the CLC from the homeotropic texture to the focal conic texture is 62 V, which is the same as that of sample C2. When the applied voltage is in the region between 62 and 75 V, the transmittance decreases with increasing voltage. When the applied voltage is higher than 75 V, the transmittance increases with increasing voltage. When the applied voltage is decreased, the CLC remains in the focal conic texture and the transmittance decreases. When the voltage is decreased to 0, the CLC is still in the focal conic state with a transmittance of 5.4%, which is higher than that of sample C2, because its focal conic domain size is larger than that of sample C2, and thus, the material has less scattering. For sample C3, the chiral dopant concentration is 10%, and the corresponding pitch is $P = 1/[8\ \mu\text{m}^{-1} \times 0.10] = 1.3\ \mu\text{m}$. Its transmittance is 85.1% at 0 V, similar to that of sample C2, but higher than that of sample C1. Under increasing applied voltage, its electro-optical behavior is similar to that of sample C2. When the applied voltage is decreased, the CLC also remains in the focal conic texture and the transmittance decreases. When the voltage is decreased to 0, the transmittance is 12.1%, which is higher than those of samples C1 and C2, probably because its focal conic domain size is too small and the scattering capability of green light becomes weaker.

When the CLC is initially in the focal conic state and the frequency of the applied voltage is 1 kHz, the results are shown in Fig. 5(b). When the voltage is applied, the CLC is switched from the focal conic texture to the homeotropic texture. When the voltage is turned OFF, the CLC remains in the homeotropic texture. The electro-optical behaviors of samples C1, C2, and C3 are similar, except the threshold voltages to switch the CLCs to the homeotropic texture are different. For samples C1 and C2, the threshold voltage is 35 V, while for sample C3, the threshold voltage is 43 V. With the consideration of the contrast ratio between the transmittances of the homeotropic texture and the focal conic texture at 0 V and the voltages to switch

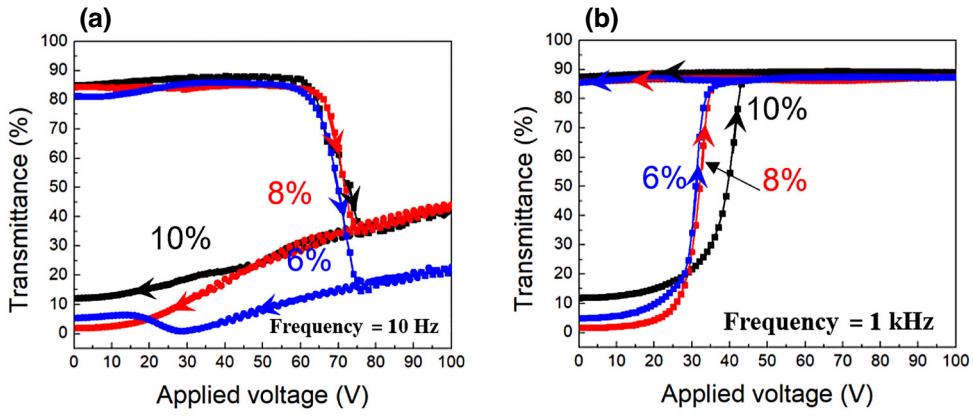

FIG. 5. Transmittance versus applied voltage curves of bistable samples with various chiral dopant (CB15) concentrations. (a) Frequency of applied voltage is 10 Hz, (b) frequency of applied voltage is 1 kHz.

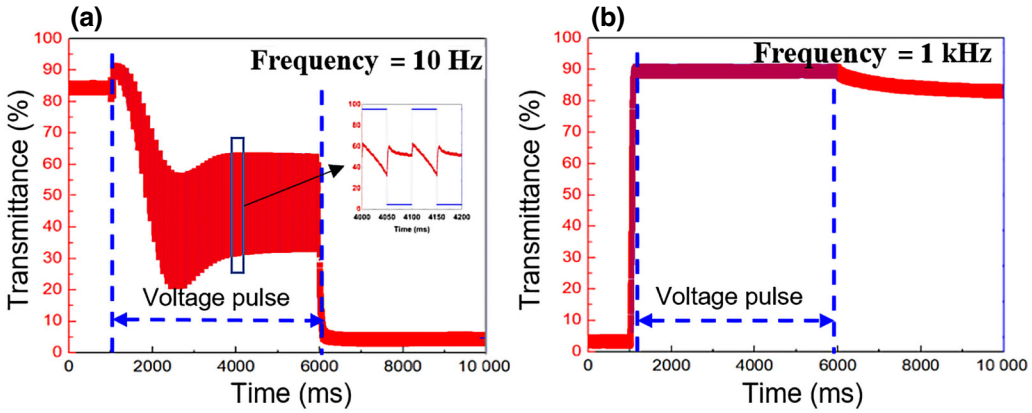

FIG. 6. Transmittance versus time when the bistable sample is switched from one state to another. (a) From the homeotropic texture to the focal conic texture, the frequency and amplitude of the applied voltage pulse are 10 Hz and 100 V, respectively. (b) From the focal conic texture to the homeotropic texture, the frequency and amplitude of the applied voltage pulse are 1 kHz and 100 V, respectively.

the CLC between the two textures, 8% chiral dopant is the best.

In real applications, smart switchable windows are usually switched by voltage pulses. We studied the response of the bistable window to voltage pulses with different frequencies. Sample R3, which performed best, was used in the study. The time width and amplitude of the square-wave voltage pulses are 5000 ms and 100 V, respectively. When the sample is switched from the homeotropic texture to the focal conic texture by the voltage pulse with a frequency of 10 Hz, the results are shown in Fig. 6(a). The pulse is turned ON at 1000 ms and turned OFF at 6000 ms. During the pulse, the transmittance oscillates with time, because the flexoelectric interaction is sensitive to the polarity of the voltage. The inset in Fig. 6(a) shows the transmittance versus time curve in the region from 4000 to 4200 ms. When the pulse is turned ON, the average transmittance decreases first. The switching time from the homeotropic texture to the focal conic texture is about 1500 ms. Then, the average transmittance becomes stable at 45%. When the pulse is turned OFF, the transmittance decreases to 2.0%, which is lower than that of the state under the applied voltage, because the domain size is decreased and the material becomes more scattering. When the sample is switched from the focal conic texture to the homeotropic texture by the voltage pulse with a frequency of 1 kHz, the results are shown in Fig. 6(b). The pulse is turned ON at 1000 ms and turned OFF at 6000 ms. The CLC is switched from the focal conic texture to the homeotropic texture in a few tens of milliseconds. The transmittance does not oscillate with time, because, at this high frequency, only the dielectric interaction (which is not sensitive to the polarity of the voltage), but not the flexoelectric interaction, affects the state of the CLC. During the pulse, the transmittance is 88%. When the pulse is turned OFF, the transmittance decreases slightly

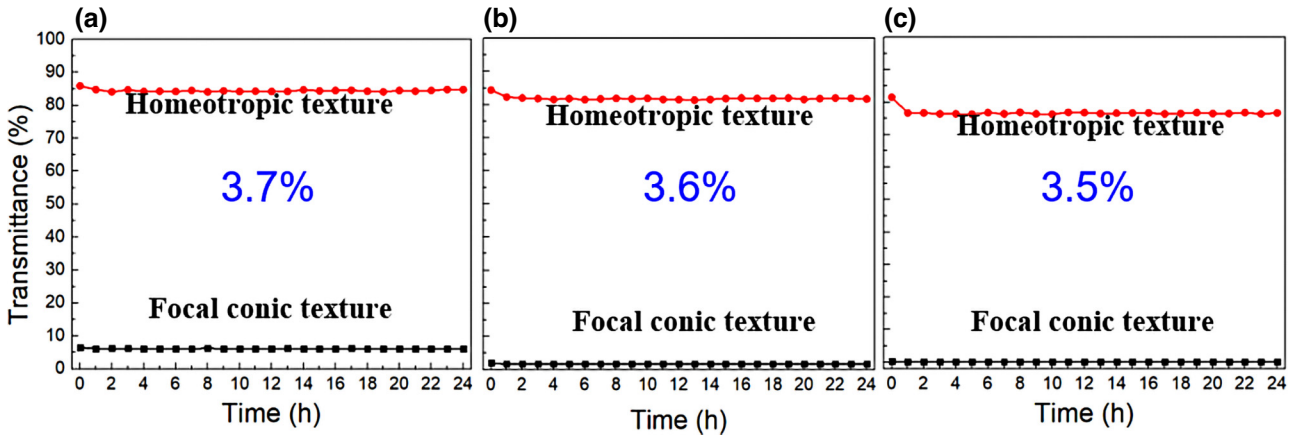

FIG. 7. Transmittance versus relaxation time of the bistable samples with various polymer-network concentrations. (a) Sample with 3.7% polymer. (b) Sample with 3.6% polymer. (c) Sample with 3.5% polymer.

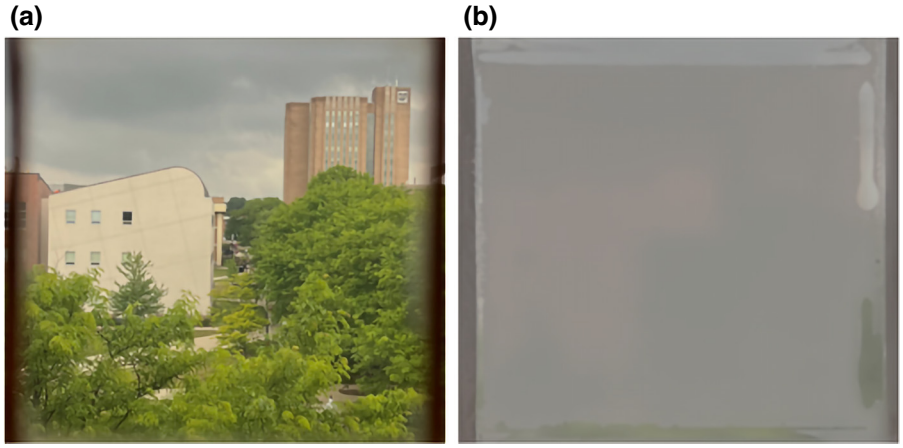

FIG. 8. Photographs of the bistable window. (a) Transparent homeotropic texture at 0 V. (b) Scattering focal conic texture at 0 V.

to 84.4%. Note that the transmittance of the transparent state at 0 V obtained by the high-frequency voltage pulse is the highest, while the transmittance of the scattering state at 0 V obtained by the low-frequency voltage pulse may not be the lowest. The transmittance of the scattering state might be further optimized by varying the amplitude of the voltage pulse. Herein, for the purpose of simplicity, the same amplitude and time interval, but different frequencies, are used for the high-frequency and low-frequency voltage pulses.

We also investigated the long-term stability of the transparent homeotropic texture and scattering focal conic texture at 0 V. Samples R2, R3, and R4 are used in the experiment. Their transmittances of the transparent and scattering states at 0 V are monitored over a period of 24 h. The results are shown in Fig. 7. For sample R2, the polymer-network concentration is 3.7%. After it is switched to the homeotropic texture by the high-frequency voltage, the transmittance initially is 85.9%. It decreases slightly to 84.8% in about 1 h and remains unchanged afterward. After it is switched to the focal conic texture by the low-frequency voltage, the transmittance initially is 6.5%. It decreases slightly to 6.1% in 24 h. For sample R3, the polymer-network concentration is 3.6%. After it is switched to the homeotropic texture by the high-frequency voltage, the transmittance initially is 84.4%. It decreases to 81.6% in about 1 h and remains unchanged afterward. After it is switched to the focal conic texture by the low-frequency voltage, the transmittance initially is 2.0%. It decreases slightly to 1.7% in 24 h. For sample R4, the polymer-network concentration is 3.5%. After it is switched to the homeotropic texture by the high-frequency voltage, the transmittance initially is 81.5%. It decreases slightly to 76.7% in about 1 h and remains unchanged afterward. After it is switched to the focal conic texture by the low-frequency voltage, the transmittance initially is 0.2%. It decreases slightly to 0.1% in 24 h. For all samples, the scattering focal conic texture is very stable. Regarding the transparent homeotropic texture, when the polymer-network concentration is high, the stability is better.

We fabricated a $2 \times 2\text{-inch}^2$ bistable window with the material of sample R3. We placed the bistable window on an architectural window and examined its performance visually. Photographs of the bistable window in the two bistable states at 0 V are shown in Fig. 8. When the window is in the transparent state, outside scenes can be seen clearly through it, as shown in Fig. 8(a). When it is in the scattering state, it completely blocks the outside scenes, as shown in Fig. 8(b). In addition, the spatial uniformity is excellent and the contrast between the two states is high.

V. CONCLUSION AND DISCUSSION

The bistable CLC switchable window exhibits two optically contrasting states in the absence of an applied voltage: one is the homeotropic texture (state), where the liquid-crystal molecules are uniformly aligned, and thus, the material is transparent, and the other is the focal conic texture (state), where the liquid-crystal molecules are in a random polydomain state, and thus, the material is scattering. The CLC has a positive dielectric anisotropy and large flexoelectric coefficients. It interacts with externally applied electric fields through both the dielectric interaction and the flexoelectric interaction. Under the dielectric interaction, the LC molecules tend to align parallel to the externally applied electric field, while under the flexoelectric interaction, the LC molecules tend to form a nonuniform polydomain state where there are spontaneous splay and bent deformations. The flexoelectric interaction is sensitive to the polarity of applied voltage, while the dielectric interaction is not sensitive. When a low-frequency (a few tens of Hz) ac voltage is applied, the LC molecules can rotate fast enough to form opposite spontaneous splay

and bent deformations when the polarity of the applied voltage is reversed. Both the flexoelectric and dielectric interactions exist. The flexoelectric interaction is, however, stronger than the dielectric interaction. The low-frequency voltage, because of the flexoelectric interaction, drives the CLC to a polydomain structure. When a high-frequency (around 1 kHz) ac voltage is applied, the LC molecules cannot rotate fast enough, due to viscosity, to form opposite spontaneous splay and bent deformations when the polarity of the applied voltage is reversed, and thus, the flexoelectric interaction has no effect on the LC. Only the dielectric interaction is effective, under which the high-frequency voltage switches the CLC to the homeotropic state.

The bistability of the homeotropic and focal conic states at 0 V is achieved through polymer stabilization, in which a small amount of anisotropic polymer network is dispersed in the CLC. The polymer network is in the direction perpendicular to the film substrates. Although the polymer network has an aligning effect on the LC, it cannot unwind the helical structure of the LC by itself. When a high-frequency voltage is applied, the aligning effect of the polymer network and the aligning effect of the electric field under the dielectric interaction are in the same direction. They act together to unwind the helical structure and switch the CLC to the homeotropic state. When the voltage is removed, the polymer network can hold the LC in the homeotropic state. When a low-frequency voltage is applied, the aligning effect of the polymer network and the aligning effect of the electric field under the flexoelectric interaction are in different directions, so the CLC is switched to a polymer domain structure. When the voltage is removed, the polymer network cannot switch the CLC to the homeotropic state, and thus, the CLC transforms into the focal conic state.

The switching of the bistable window is accomplished by using dielectric and flexoelectric interactions. An ac voltage of low frequency in the region from 0 to 50 Hz switches the window from the transparent state to the scattering state under the flexoelectric interaction. An ac voltage of high frequency in the region from 500 to 5000 Hz switches the window from the scattering state back to the transparent state under the dielectric interaction. The required voltage amplitude of the low-frequency voltage depends slightly on the frequency of the applied voltage because the domain size changes slightly with frequency. The required voltage amplitude of the high-frequency voltage almost does not depends on the frequency of the applied voltage because the dielectric anisotropy does not change in the frequency region.

The frequency of the high-frequency voltage to switch the CLC to the homeotropic state is only 1 kHz, and thus, power consumption, due to the capacitor's impedance of the window, is much lower than that when dual-frequency liquid crystals are used. The resistivity of the CLC is high, which is another factor attributed to the low power needed for switching. In some bistable windows, ions are doped to produce electroconvective instability, which is used to switch the CLC to the focal conic state. The doped ions not only increase the power needed for switching dramatically, but also cause long-term chemical degradation of the CLC [61,62].

In summary, we developed a smart switchable CLC window of two stable states at 0 V. The optical contrast between the two states is high. The transparent state has a high transmittance of 82%, and the scattering state has a low transmittance of 2%. The window is switched between the two states by voltage pulses. The frequencies of voltage pulses for switching are low and can be easily implemented. For a smart window based on PDLCs, a continuous voltage must be applied to keep the window in the transparent state, which typically consumes power of 10 W/m^2 [63]. For our smart window, no continuously applied voltage is needed to sustain the two optical states, and thus, the window is very energy saving. The window is expected to have a significant impact on switchable architectural building and vehicle windows.

The authors declare no conflicts of interest.

[1] Marina Aburas, Veronica Soebarto, Terence Williamson, Runqi Liang, Heike Ebendorff-Heidepriem, and Yupeng Wu, Thermochromic smart window technologies for building application: A review, Appl. Energy **255**, 113522 (2019).
[2] Srijita Nundy, Abdelhakim Mesloub, Badr M. Alsolami, and Aritra Ghosh, Electrically actuated visible and near-infrared regulating switchable smart window for energy positive building: A review, J. Cleaner Prod. **301**, 126854 (2021).
[3] Jean-Michel Dussault, Louis Gosselin, and Tigran Galstian, Integration of smart windows into building design for reduction of yearly overall energy consumption and peak loads, Sol. Energy **86**, 3405 (2012).
[4] Niall R. Lynam, "Smart windows for automobiles." (1990).
[5] Carl M Lampert, Smart switchable glazing for solar energy and daylight control, Sol. Energy Mater. Sol. Cells **52**, 207 (1998).
[6] Ruben Baetens, Bjørn Petter Jelle, and Arild Gustavsen, Properties, requirements and possibilities of smart windows for dynamic daylight and solar energy control in buildings: A state-of-the-art review, Sol. Energy Mater. Sol. Cells **94**, 87 (2010).
[7] Carl M. Lampert, Large-area smart glass and integrated photovoltaics, Sol. Energy Mater. Sol. Cells **76**, 489 (2003).
[8] Aritra Ghosh, Brian Norton, and Aidan Duffy, Daylighting performance and glare calculation of a suspended particle device switchable glazing, Sol. Energy **132**, 114 (2016).
[9] Aritra Ghosh, Brian Norton, and Aidan Duffy, Effect of sky conditions on light transmission through a suspended particle device switchable glazing, Sol. Energy Mater. Sol. Cells **160**, 134 (2017).

[10] Linfeng Luo, Yinghui Liang, Yuting Feng, Dan Mo, Yang Zhang, and Jiawen Chen, Recent progress on preparation strategies of liquid crystal smart windows, Crystals **12**, 1426 (2022).
[11] Seung-Won Oh, Seong-Min Ji, Chan-Hee Han, and Tae-Hoon Yoon, A cholesteric liquid crystal smart window with a low operating voltage, Dyes Pigm. **197**, 109843 (2022).
[12] Wenbo Shen and Guoqiang Li, Recent progress in liquid crystal-based smart windows: Materials, structures, and design, Laser Photonics Rev. **17**, 2200207 (2023).
[13] Toru Ube, Jumpei Imai, Marie Yoshida, Toru Fujisawa, Hiroshi Hasebe, Haruyoshi Takatsu, and Tomiki Ikeda, Sunlight-driven smart windows with polymer/liquid crystal composites for autonomous control of optical properties, J. Mater. Chem. C **10**, 12789 (2022).
[14] A. Azens and C. Granqvist, Electrochromic smart windows: energy efficiency and device aspects, J. Solid State Electrochem. **7**, 64 (2003).
[15] Yi Liang, Sheng Cao, Juquan Guo, Ruosheng Zeng, Jialong Zhao, and Bingsuo Zou, Dual-band electrochromic smart window based on single-component nanocrystals, ACS Appl. Electron. Mater. **4**, 5109 (2022).
[16] Ting Bai, Wanzhong Li, Guoxing Fu, Qianqian Zhang, Kailing Zhou, and Hao Wang, Dual-band electrochromic smart windows towards building energy conservation, Sol. Energy Mater. Sol. Cells **256**, 112320 (2023).
[17] Daniela Cupelli, Fiore Pasquale Nicoletta, Sabrina Manfredi, Marco Vivacqua, Patrizia Formoso, Giovanni De Filpo, and Giuseppe Chidichimo, Self-adjusting smart windows based on polymer-dispersed liquid crystals, Sol. Energy Mater. Sol. Cells **93**, 2008 (2009).
[18] Li Jinqian, Yuzhen Zhao, Hong Gao, Dong Wang, Zongcheng Miao, Hui Cao, Zhou Yang, and Wanli He, Polymer dispersed liquid crystals doped with CeO_2 nanoparticles for the smart window, Liq. Cryst. **49**, 29 (2022).
[19] Mingyun Kim, Kyun Joo Park, Seunghwan Seok, Jong Min Ok, Hee-Tae Jung, Jaehoon Choe, and Do Hyun Kim, Fabrication of microcapsules for dye-doped polymer-dispersed liquid crystal-based smart windows, ACS Appl. Mater. Interfaces **7**, 17904 (2015).
[20] Saboor Shaik, Kirankumar Gorantla, Shantiswaroop Mishra, and Kishor S. Kulkarni, Thermal and cost assessment of various polymer-dispersed liquid crystal film smart windows for energy efficient buildings, Constr. Build. Mater. **263**, 120155 (2020).
[21] Waqas Kamal, Mengmeng Li, Jia-De Lin, Ellis Parry, Yihan Jin, Steve J. Elston, Alfonso A. Castrejón-Pita, and Stephen M. Morris, Spatially patterned polymer dispersed liquid crystals for image-integrated smart windows, Adv. Opt. Mater. **10**, 2101748 (2022).
[22] Abdelhakim Mesloub, Aritra Ghosh, Lioua Kolsi, and Mohammad Alshenaifi, Polymer-dispersed liquid crystal (PDLC) smart switchable windows for less-energy hungry buildings and visual comfort in hot desert climate, J. Build. Eng. **59**, 105101 (2022).
[23] J. W. Doane, N. A. Vaz, B-G Wu, and Slobodan Žumer, Field controlled light scattering from nematic microdroplets, Appl. Phys. Lett. **48**, 269 (1986).
[24] Yang Zhang, Changrui Wang, Wei Zhao, Ming Li, Xiao Wang, Xiulan Yang, Xiaowen Hu, *et al.*, Polymer stabilized liquid crystal smart window with flexible substrates based on low-temperature treatment of polyamide acid technology, Polymers **11**, 1869 (2019).
[25] D. J. Broer, R. G. Gossink, and R. A. M. Hikmet, Oriented polymer networks obtained by photopolymerization of liquid-crystalline monomers, Angew. Makromol. Chem.: Appl. Macromol. Chem. Phys. **183**, 45 (1990).
[26] D. J. Broer, in *Liquid Crystals in Complex Geometries: Formed by Polymer and Porous Networks*, edited by G. P. Crawford and S. Zumer (CRC press, Boca Raton, FL, 1996), p. 239.
[27] R. A. M. Hikmet, in *Liquid Crystals In Complex Geometries: Formed by Polymer and Porous Networks*, edited by G. P. Crawford and S. Zumer (CRC Press, Boca Raton, FL, 1996), p. 53.
[28] Yang Zhang, Jiawen Chen, Xiaowen Hu, Wei Zhao, Dirk Broer, and Guofu Zhou, Reverse mode polymer dispersed liquid crystal-based smart windows: A progress report, Recent Prog. Mater. **3**, 1 (2021).
[29] D-K Yang, L-C Chien, and J. W. Doane, Cholesteric liquid crystal/polymer dispersion for haze-free light shutters, Appl. Phys. Lett. **60**, 3102 (1992).
[30] Xiaoyu Jin, Yuning Hao, Zhuo Su, Ming Li, Guofu Zhou, and Xiaowen Hu, Dual-function smart windows using polymer stabilized cholesteric liquid crystal driven with interdigitated electrodes, Polymers **15**, 1734 (2023).
[31] Andy Ying-Guey Fuh, Zong Bai Shin, Ching Han Yang, and Shing-Trong Wu, Electrically controllable smart window with greyscale based on polymer-stabilised cholesteric texture films, Liq. Cryst. **43**, 1784 (2016).
[32] Deng-Ke Yang, in *Liquid Crystals Beyond Displays: Chemistry, Physics, and Applications*, edited by Quan Li (John Wiley & Sons, Chichester, Hoboken, NJ, 2012), p. 505.
[33] Kyung Min Lee, Vincent P. Tondiglia, and Timothy J. White, Bistable switching of polymer stabilized cholesteric liquid crystals between transparent and scattering modes, MRS Commun. **5**, 223 (2015).
[34] Farzana Ahmad, Muhammad Jamil, and Young Jae Jeon, Reverse mode polymer stabilized cholesteric texture (PSCT) light shutter display-a short review, J. Mol. Liq. **233**, 187 (2017).
[35] Huimin Zhang, Jie Liu, Xiangrong Zhao, Jianjing Gao, Cheng Ma, Yang Zhao, Ruijuan Yao, Zongcheng Miao, and Wenbo Shen, Electrically induced coloration of polymer-stabilized cholesteric liquid crystal films with broadband reflection capability for smart windows, Dyes Pigm. **203**, 110316 (2022).
[36] Deng-Ke Yang and Shin-Tson Wu, *Fundamentals of Liquid Crystal Devices* (John Wiley & Sons, Chichester, Hoboken, NJ, 2014).
[37] Paul S. Drzaic, *Liquid Crystal Dispersions* (World scientific, Hackensack, NJ, 1995).
[38] Alireza Moheghi, Hossein Nemati, Yannian Li, Quan Li, and Deng-Ke Yang, Bistable salt doped cholesteric liquid crystals light shutter, Opt. Mater. **52**, 219 (2016).
[39] Cheng-Chang Li, Heng-Yi Tseng, Chun-Wei Chen, Chun-Ta Wang, Hung-Chang Jau, Yu-Ching Wu, Wen-Hao Hsu, and Tsung-Hsien Lin, Versatile energy-saving smart glass

based on tristable cholesteric liquid crystals, ACS Appl. Energy Mater. **3**, 7601 (2020).
[40] Ji Ma, Lei Shi, and Deng-Ke Yang, Bistable polymer stabilized cholesteric texture light shutter, Appl. Phys. Express **3**, 021702 (2010).
[41] Chien-Hui Wen and Shin-Tson Wu, Dielectric heating effects of dual-frequency liquid crystals, Appl. Phys. Lett. **86**, 231104 (2005).
[42] M. Schadt, Dielectric heating and relaxations in nematic liquid crystals, Mol. Cryst. Liq. Cryst. **66**, 319 (1981).
[43] P. G. De Gennes and J. Prost, *The Physics of Liquid Crystals* (Oxford Univ. Press, New York, 1995).
[44] N. Éber, P. Salamon, and Á Buka, Electrically induced patterns in nematics and how to avoid them, Liq. Cryst. Rev. **4**, 101 (2016).
[45] R. B. Meyer, Piezoelectric effects in liquid crystals, Phys. Rev. Lett. **22**, 918 (1969).
[46] Y. Jiang, X. Zhou, G. Qin, X. Xu, S. Lee, and D.-K. Yang, Effects of flexoelectricity and ion on the flicker of fringe field switching liquid crystal display, SID Symp. Dig. Tech. Pap. **49**, 1095 (2018).
[47] J. S. Patel and R. B. Meyer, Flexoelectric electro-optics of a cholesteric liquid crystal, Phys. Rev. Lett. **58**, 1538 (1987).
[48] J. Harden, B. Mbanga, N. Éber, K. F. Csorba, S. Sprunt, J. T. Gleeson, and Antal Jakli, Giant flexoelectricity of bent-core nematic liquid crystals, Phys. Rev. Lett. **97**, 157802 (2006).
[49] Meina Yu, Ling Wang, Hossein Nemati, Huai Yang, Timothy Bunning, and Deng-Ke Yang, Effects of polymer network on electrically induced reflection band broadening of cholesteric liquid crystals, J. Polym. Sci., Part B: Polym. Phys. **55**, 835 (2017).
[50] Deng-Ke Yang, Yue Cui, Hossein Nemati, Xiaochen Zhou, and Alireza Moheghi, Modeling aligning effect of polymer network in polymer stabilized nematic liquid crystals, J. Appl. Phys. **114**, 243515 (2013).
[51] M. Cestari, S. Diez-Berart, D. A. Dunmur, A. Ferrarini, M. R. De La Fuente, D. J. B. Jackson, D. O. Lopez, G. R. Luckhurst, M. A. Perez-Jubindo, R. M. Richardson, and J. Salud, Phase behavior and properties of the liquid-crystal dimer 1″, 7″-bis (4-cyanobiphenyl-4′-yl) heptane: A twist-bend nematic liquid crystal, Phys. Rev. E **84**, 031704 (2011).
[52] V. Borshch, Y.-K. Kim, J. Xiang, M. Gao, A. Jákli, V. P. Panov, J. K. Vij, C. T. Imrie, M. G. Tamba, G. H. Mehl, and O. D. Lavrentovich, Nematic twist-bend phase with nanoscale modulation of molecular orientation, Nat. Commun. **4**, 1 (2013).
[53] D. Chen, J. H. Porada, J. B. Hooper, A. Klittnick, Y. Shen, M. R. Tuchband, E. Korblova, D. Bedrov, D. M. Walba, M. A. Glaser, and J. E. Maclennan, Chiral heliconical ground state of nanoscale pitch in a nematic liquid crystal of achiral molecular dimers, Proc. Natl. Acad. Sci. U. S. A. **110**, 15931 (2013).
[54] Greta Babakhanova, Zeinab Parsouzi, Sathyanarayana Paladugu, Hao Wang, Yu. A. Nastishin, Sergij V. Shiyanovskii, Samuel Sprunt, and Oleg D. Lavrentovich, Elastic and viscous properties of the nematic dimer CB7CB, Phys. Rev. E **96**, 062704 (2017).
[55] Andrii Varanytsia and Liang-Chy Chien, Giant flexoelectro-optic effect with liquid crystal dimer CB7CB, Sci. Rep. **7**, 41333 (2017).
[56] Yingfei Jiang, Xiaochen Zhou, Yunho Shin, Guangkui Qin, Xiaoguang Xu, Li Zhou, SeungHee Lee, and Deng-Ke Yang, Image flickering reduction by dimer and polymer stabilization in FFS liquid crystal display, J. Soc. Inf. Disp. **27**, 285 (2019).
[57] Yunho Shin, Ziyuan Zhou, Suman Halder, Xinfang Zhang, and Deng-Ke Yang, Reconfigurable liquid crystal diffraction grating based on flexoelectric effect, J. Mol. Liq. **357**, 119150 (2022).
[58] Ying Xiang, Hong-Zhen Jing, Zhi-Dong Zhang, Wen-Jiang Ye, Ming-Ya Xu, Everett Wang, Péter Salamon, Nándor Éber, and Ágnes Buka, Tunable optical grating based on the flexoelectric effect in a bent-core nematic liquid crystal, Phys. Rev. Appl. **7**, 064032 (2017).
[59] Rui Yuan, Wen-Jiang Ye, Hong-Yu Xing, Zhen-Jie Li, Ting-Ting Sun, Yu-Bao Sun, Ji-Liang Zhu, Ying Xiang, Zhi-Yong Zhang, and Ming-Lei Cai, Continuously adjustable period optical grating based on flexoelectric effect of a bent-core nematic liquid crystal in planar cells, Opt. Express **26**, 4288 (2018).
[60] Nándor Éber, Ying Xiang, and Ágnes Buka, Bent core nematics as optical gratings, J. Mol. Liq. **267**, 436 (2018).
[61] S. H. Perlmutter, D. Doroski, and G. Moddela, Degradation of liquid crystal device performance due to selective adsorption of ions, Appl. Phys. Lett. **69**, 26 (1996).
[62] Jeong-Ho Seo, Jae-Won Huh, Ho-Jin Sohn, Eunjung Lim, and Tae-Hoon Yoon, Analysis of optical performance degradation in an ion-doped liquid-crystal cell with electrical circuit modeling, Crystals **10**, 55 (2020).
[63] M. S. Islam, K.-Y. Chan, G. S. H. Thien, P.-L. Low, C.-L. Lee, S. K. Wong, E. E. Mhd Noor, B. W.-C. Au, and Z.-N. Ng, Performances of polymer-dispersed liquid crystal films for smart glass applications, Polymers **15**, 3420 (2023).